CASE STUDY

Phase Transformations in Chiral Non-racemic Main-chain Liquid Crystalline Polyesters Involving Double-twist Helical Crystals

Authors:

Christopher Y. Li,[1] Shi Jin,[2] Xin Weng,[2] Dong Zhang,[2] Feng Bai,[2] John Z. Zhang,[2] Frank W. Harris,[2] Liang-Chy Chien,[3] Bernard Lotz[4] and Stephen Z. D. Cheng[2]*

[1] Department of Materials Science and Engineering, Drexel University, Philadelphia, Pennsylvania 19104

[2] The Maurice Morton Institute and Department of Polymer Science, The University of Akron, Akron, Ohio 44325-3909

[3] Liquid Crystal Institute, Kent State University, Kent, Ohio

[4] Institute Charles Sadron, 6 Rue Boussingault, Strasbourg

* Correspondence should be addressed to: chrisli@drexel.edu and scheng@uakron.edu

Abstract

It is for the first time the double-twisted helical single lamellar crystals were observed in a series of synthetic chiral non-racemic main-chain liquid crystalline polyesters. Phase structure and transition behaviors were investigated. Multiple liquid crystalline phases were found including the twisted grain boundary phase. During crystallization, the chain molecules kept their memory of the primary and secondary chiral structures, and transferred to the tertiary chiral structure. The hierarchies of these chiralities in different length scales were also discussed.

Chiralities in Different Length Scales

Chirality in molecules has generated profound new phase structures, transition behaviors and specific optical and electric properties in low molecular mass liquid crystals, biomacromolecules and synthetic polymers.[1-5] In polymer systems, due to their long chain nature, chirality can be defined in different length scales forming the chirality "hierarchies" as shown in Figure 1.[6] Asymmetrical chiral centers introduced into a polymer backbone, which is a primary chiral structure (configurational chirality), usually result in helical macromolecular conformations (a secondary chiral structure, conformational chirality). When the polymer chains with helical conformations pack together following symmetry operations to form ordered structures, the chirality may break the local mirror symmetry and lead to a helical morphology (a tertiary chiral structure, phase chirality) depending on the type of structural ordering formed. The helical lamellae usually aggregate together to banded spherulites due to cooperative lamellar twisting, and it is identified as quaternary chiral structure, which can be defined as the object chirality as shown in Figure 1.

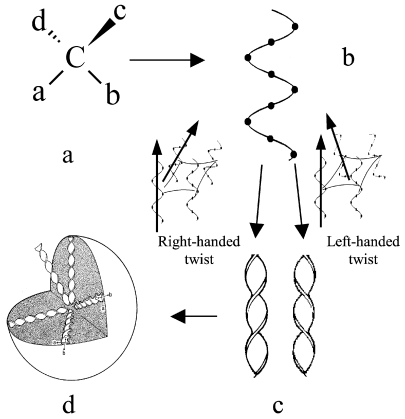

Figure 1. Four levels of chirality in polymers.

It has been recognized that attempts to relate the primary chiral structure with the quaternary one without knowing the secondary and tertiary chiral structures is an incomplete practice.[6-10] In other words, *transferring from one chirality hierarchy to another need be neither automatic nor necessary.* Establishing quantitative links between the configurational chirality and objective chirality requires information on the conformational and phase chiralities.

In the past several years, we have focused on the study of a series of non-racemic chiral main-chain liquid crystalline (LC) polyester synthesized from (R)-(-)-4'-{ω-[2-(*p*-hydroxy-*o*-nitrophenyloxy)-1-propyloxy]-1-nonyloxy}-4-biphenyl carboxylic acid, abbreviated PET(R*)-n, where n is the number of methlene units.[6-10]

This series of polymer possesses right-hand chiral centers (R*) along the main-chain backbones. Due to the head-to-tail connection of the monomers in this polymer (an A-B monomer polymerization),[10] the optical activity of the monomers are retained, and, the polymers are non-racemic. The molecular weights of PET(R*)-n are around 16k - 25k g/mol and the polydispersity is approximately 2 after fractionations, as measured by gel permeation chromatography based on polystyrene standards.

For the first time, both flat-elongated and helical single lamellar crystals have been thermotropically grown under the same crystallization condition, and the helical crystal is shown in Figure 3.[6-9] Base on our electron diffraction (ED) experiments, surprisingly, these crystals possess the same structure. Polymer chain folding directions in both flat and helical lamellar crystals have also been determined to be identical, and it is always along the long axis of the lamellar crystals.[6-9]

Recent dark field (DF) image, bright field image, and selective area electron diffraction (SAED) experiments in transmission electron microscopy (TEM) provide chain orientation information for the helical lamellar crystals.[6,9] It has been found that the main twist direction is parallel to the long helical axis, and the rotating angle for each molecular layer is approximately 0.05°.[6,9] Specifically designed DF experiments using the entire and partial (205) and (206) diffraction arcs show that the chain orientation direction is also twisted along the short helical axis of the lamellar crystal. The rotating angle is approximately 0.01° per molecular layer. This leads to a second twist direction in addition to the twist along the long helical axis of the crystal.[6,9] Based on these experimental observations, the concept of *double-twist* molecular orientation in the helical lamellar crystal can be established, although in principle, the macroscopic translation symmetry is broken along both the long and short axes of the helical lamellar crystals. This crystal can therefore be recognized as symmetrically "soft", rather than a true crystal based on the traditional crystal definition in Euclidean space. Mathematically, double-twist crystals can only be true crystals in Riemannian space.[6,9]

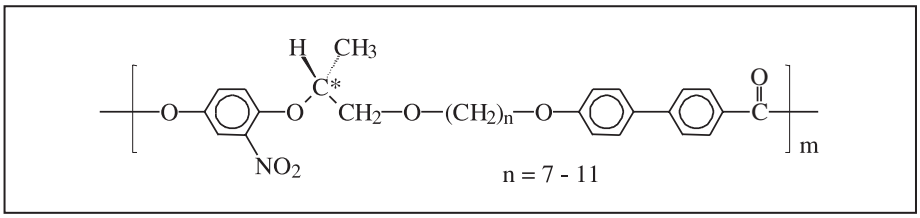

Figure 2. The general polymer repeat unit chemical structure.

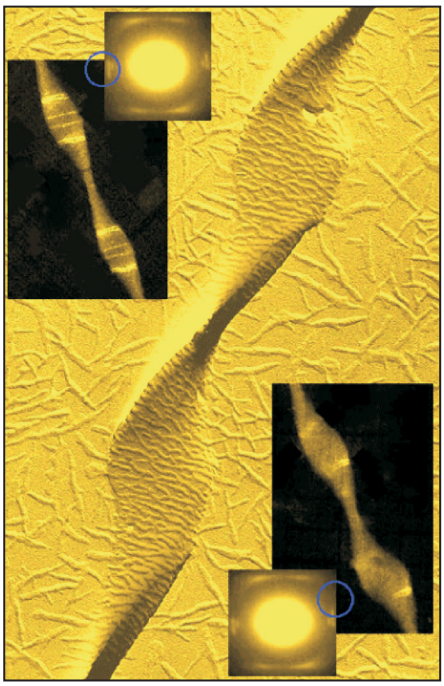

Figure 3. A right-handed lamellar helical crystal of PET (R*-9) with DF and SAED results to provide evidence of double-twisted molecular arrangement in the crystal.

Upon careful examination of the crystallization behaviors of PET(R*)-n, it is not difficult to find that the crystallization takes place in a LC phase instead of the isotropic melt. The crystallization behaviors and crystal morphologies formed may critically depend upon the molecular orientation and structural order in this LC phase. Therefore, a clear understanding of the phase structures and transformations of this series of polymers is necessary in order to establish connections among the chiralities in different length scales.

Thermodynamic Transition Behaviors

Figures 4a and 4b show a set of cooling and subsequent heating DSC thermal diagrams for PET(R*)-9 at different rates between 2.5 °C/min and 40 °C/min, as an example. A glass transition temperature (T_g) at 37 °C is evident. When the cooling and heating rates are equal or faster than 10 °C/min, there is apparently a first-order transition appearing at an onset transition temperature of 185 °C during cooling and 175 °C during heating. Of interest is that the onset transition temperature during cooling is higher than during heating. This is a possible indication of two overlapped first-order transitions or a bi-phasic phenomenon. If one uses a slower cooling rate of 0.5 °C/min, two separated first-order transitions start to be observed (the insert of Figure 4a). In fact, this type of observation has also been found in other LC polymers, as recently reported.[11] The enthalpy changes of these two first-order transitions are 3.21 kJ/mol (for the higher temperature transition) and 1.27 kJ/mol (for the lower temperature transition), respectively. Another transition can be found at 130 °C with a small transition

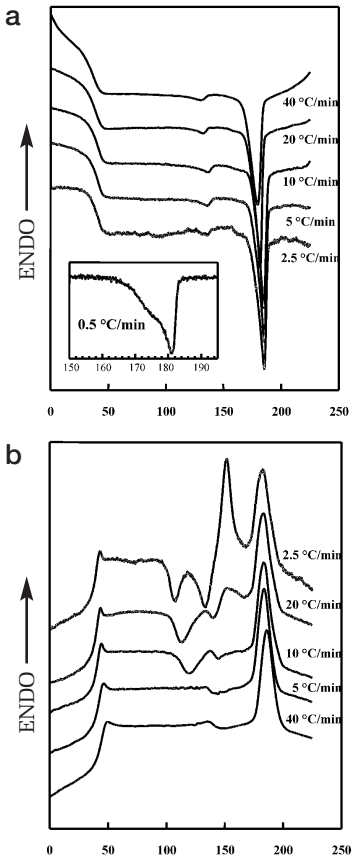

Figure 4. DSC cooling (a) and heating (b) thermodigrams at different rates between 0.5 and 40°C/min.

enthalpy change (0.35 kJ/mol). All three transitions are almost cooling and heating rate independent in the range of rates investigated, indicating that these transitions are associated with LC phase transformations, which are close to thermodynamic equilibrium.

When the DSC controlled heating rates are slower than 10 °C/min, additional thermal events take place. These transitions must be attributed to crystallization and melting of the crystals in this polymer since their transition temperatures and enthalpy changes are very much cooling and heating rate dependent. This is indicative of kinetically controlled transition processes.

Identification of LC Phases

Figure 5 shows a set of one-dimensional (1D) WAXD patterns during a fast cooling from the isotropic melt to room temperature at a rate of 20 °C/min. The LC phases certainly cannot be by passed at this cooling rate due to the near thermodynamic equilibrium nature. The 1D WAXD pattern at 190 °C shows evidence of a transition characterized by two features. The first is the appearance of a low-angle reflection at 2θ = 3.0° (d-spacing of 2.96 nm). The second is a sudden shift of the wide-angle halo at around 2θ = 20°. Both features indicate a transition from the isotropic melt to a low ordered smectic LC phase.[11-15] When the temperature is continuously decreased to 130 °C, the low-angle reflection exhibits a shift to a slightly higher angle of 2θ = 3.05° (d-spacing of 2.90 nm). Furthermore, the wide-angle scattering halo becomes increasingly sharper on cooling to 130 °C. Note that this transition can also be found in the DSC cooling and heating thermal diagrams (Figure 4). After we conducted 2D WAXD experiments at different temperatures, it is found that at 160 °C the LC phase is a typical smectic A (S_A) phase since the layer reflection from the low-angle is on the equator and the scattering halo is on the meridian. After annealing at 120 °C, however, the 2D WAXD pattern shows that the scattering halo is still on the meridian while the layer reflection is slightly shifted to the quadrant, which is a typical S_C pattern. The angle between the layer reflection and the meridian (the fiber direction) is 79°, indicating that the layer normal is tilted 11° away from the equator. Therefore, the transition at 130 °C is a $S_A^* \leftrightarrow S_C^*$ transition.

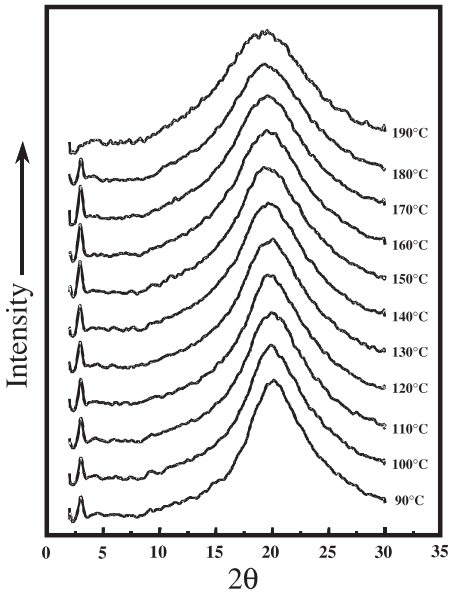

Figure 5. 1D WAXD patterns at different temperatures during cooling at 20 °C/min rate.

The assignments of S_A^* and S_C^* are also supported by texture observations under PLM at different temperatures. The sample was sheared and relaxed at 180 °C and then slowly (1 °C/min) cooled and annealed at 160 °C and 120 °C. Figure 6a shows a S_A^* focal conic texture formed after the sheared sample was annealed at 160 °C, while this texture is broken when cooled down passing 130 °C at which the phase transition takes place (Figure 6b). The broken focal conics are indicative of the S_C^* phase which is consistent with X-ray fiber pattern results. The formation of this texture is due to the shrinkage of layer thickness during the transition.

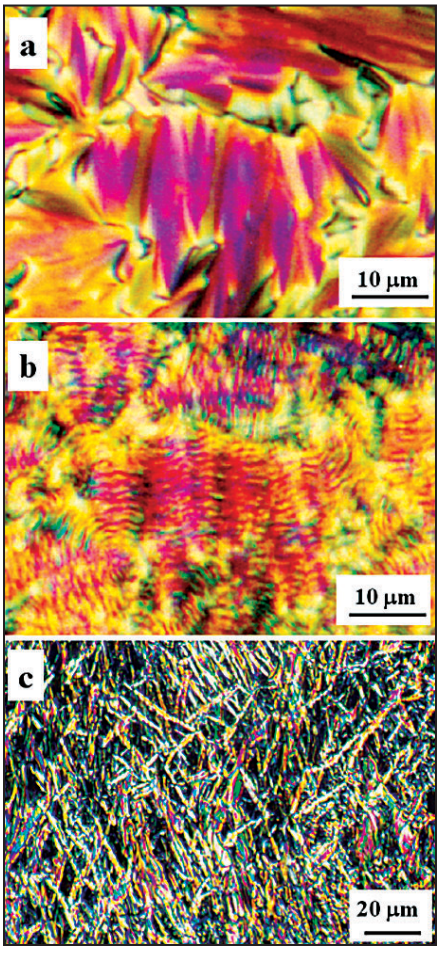

Figure 6. PLM pictures of S_A^*, S_C^* and TGBA phases.

The remaining issue is the overlapped transition that occurs between 175 °C and 185 °C which should be associated with the third phase. Note that the highest temperature phase is the isotropic melt, while below 175 °C it is the S_A* phase. Based on the WAXD results, one can conclude that this undetermined phase must also be related to the S_A* phase since the low angle reflection at $2\theta = 3.0°$, which represents the layer structure, starts to appear at 185 °C, and in fiber heating experiments, the layer reflection does not disappear until 185 °C. However, neither the WAXD powder nor the fiber patterns are sensitive to the structure changes of this transition; one speculates that this transition must be related to the larger length scale of supra-molecular assembly rather than structures on the molecular level. The observations obtained by PLM show helical textures with alternating strong and weak birefringence as shown in Figure 6c. This LC morphology is virtually identical to the twisted grain boundary (TGB) phase morphology observed in small molecule LC and side-chain LC polymers.[16,17] Combining both observations of the PLM helical texture and the WAXD results, it is strongly suggested that the high temperature phase mediate isotropic melt and the S_A* phase is a TGBA* phase.

Identification of Crystalline Phase

In principle, crystallization occurs between the T_g and T_m, and therefore, for this polymer, the crystallization window should be between 37 °C and 170 °C. However, the S_A* phase is in the temperature region of 130 °C to 175 °C, while the temperature region between 37 °C and 130 °C is the S_C* phase. As shown in Figures 4, when the heating rate is slow (≤ 5 °C/min), crystallization takes place. Figure 7 shows a set of WAXD powder patterns recorded during heating at 1 °C/min for a quenched PET(R*)-9 sample. When the temperature reaches 80 °C, multiple reflections start to appear in the wide-angle region, indicating that crystallization is initiated. These reflections remain until the temperature approaches 170 °C, at which the crystal melts. The focus here is only on the crystal structure developed from the S_A* phase.

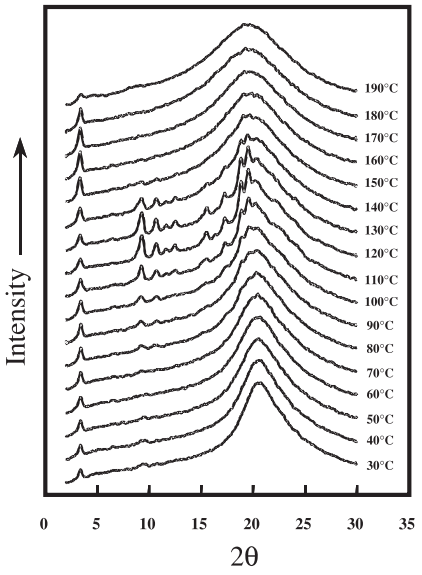

Figure 7. A set of 1D WAXD pattern at different temperatures under a heating rate of 1 °C/min for a quenched PET(R*)-9 sample.

The crystal structure can be determined using both the SAED and WAXD techniques. Figure 8a shows a 2D WAXD pattern that has been annealed at 145 °C for one day and then quenched to room temperature. It is evident that multiple reflections can be seen. First, along the equator, reflections up to the sixth order appear, corresponding to the (00*l*) planes. Therefore, the c-axis dimension can be determined to be 5.96 nm, in excellent agreement with the results derived from SAED experiments.[7,8] This indicates that the fiber direction is perpendicular to the chain direction, similar to many biopolymer fibers.[18] However, in biopolymers, this kind of molecular orientation in the fibers is perhaps due to the existence of the parallel and anti-parallel hydrogen bond interactions between the chain molecules and their supra-molecularly assembled β-pleated sheets. On the other hand, the origin of this anomalous 2D WAXD pattern may be associated with the fact that the fibers were drawn from the S_A* phase, similar to the example of a series of poly(ester imide)s reported recently.[19]

The fiber meridian can be assigned as the a* direction. In the quadrants, there are three layers of reflections that can be observed. For example, the first (1kl) layer [instead of (hk1) in a normal polymer fiber pattern since the fiber direction is defined as the a*-direction] possesses six reflections. In the second (2kl) layer four reflections are observed. The third (3kl) layer has one reflection, *etc.* Of interest is that the (h1l) reflections are relatively diffused in Figure 8 (see arrows in the figure), which are possibly due to the superstructure formation as discussed in previous publications.[7,8] Figure 8b is an ED pattern for sheared samples, showing the a*c* reciprocal plane. The (h1l) arcs in the fiber pattern can not be observed in Figure 7b because the sheared ED pattern only presents the a*c* reciprocal plane, consisting of (h0l) diffractions. After careful refinement of the WAXD fiber reflections, the crystal lattice can be determined to be orthorhombic with dimensions of a = 10.7 nm, b = 0.48 nm and c = 5.96 nm. This result is in excellent agreement with that determined via the SAED technique.[6-9]

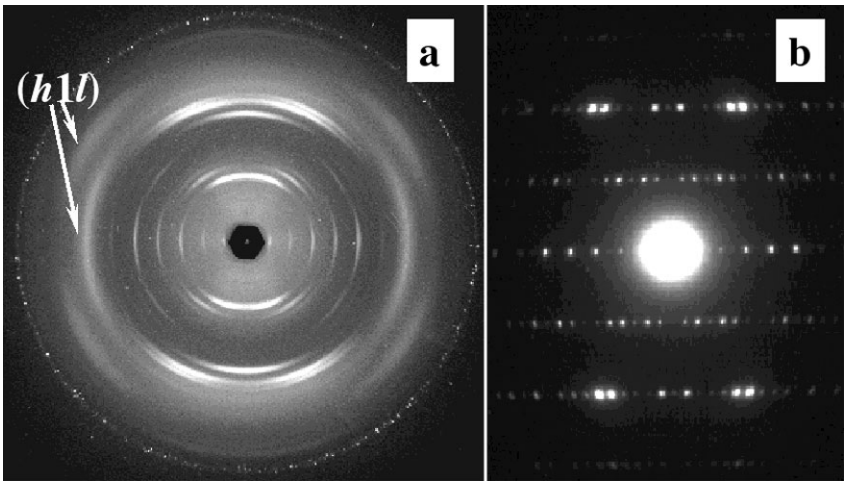

Figure 8. A 2D WAXD pattern (a) and a SAED pattern (b).

When crystallization is carried out in the S_A* phase, both flat-elongated and helical single lamellar crystals can be formed. Surprisingly enough, the crystal structures of these two crystals are identical. Polyethylene decoration on the surface of the crystals shows that the chain folding direction is along the long axis of the crystals. This reveals that the chain folds towards the less ordered S_A phase rather than along the crystalline planes.[6-9] Therefore, this adds a new factor to the discussion of the crystal growth mechanism of these crystals in the near future. Other findings indicate that not only the lamellar crystal thickness but the length of periodicity as well increase with crystallization temperature. Furthermore, the observations of flat and helical lamellar crystals also suggests that the free energies of forming the flat and helical molecular packing may be comparable, and therefore, both of the morphologies can be observed.[6-9]

Combining the phase transition behaviors with the double-twist chain orientation in the helical lamellar crystals, a remarkable similarity of this polymer with biomacromoleculescan be seen,[20-24] although no hydrogen bonds exist in PET(R*)-9. Some biomacromolecules possess the double-twisted helical packing in LC states rather than in a three dimensionally ordered crystal, such as in the case of dinoflagellate chromosomes (in *Prorocentrum micans*) which displays the same type of helical structure in an *in vivo* arrangement.[20-22] *Bombyx mori* silk fibroin can grow a helical lamellar crystal of the β-modification under solution crystallization conditions.[24] Hopefully, the study of the structure, morphology and phase transitions of PET(R*)-9 will initiate a new step in understanding biopolymer behaviors in responses to various environments.

Odd-Even Effects on Different Structural Length Scales

In the case of PET(R*-9), the helical lamellar crystals possess a right-handedness. This is for all the PET(R*)-n when n is odd numbers (n = 7, 9, and 11). However, when the n = even numbers of 8 and 10, The helical handedness turns to left-handedness. In other words, the helical handedness can also show odd-even effect. This observation clearly indicates that the molecular chirality is important, but not the only factor to consider in determining the chirality on the large length scales. We have demonstrated that the chirality transformation is determined most critically by *the pack scheme of the building blocks on each structural length scales*.[23] This effect must be attributed to the molecular conformation differences between these two sets of LC homologues, although specific structural packing schemes were not determined.

After examining this series of PET(R*)-n (n = 7 -11), we observed profound odd-even effects in different length scales. This effect was found not only on the helical handedness as we just described, but also from crystal unit cell lattice length scale to thermodynamic transition properties. In the unit cell length scale, the PETs(R*-odd) possessed monoclinic cells with a c axis having a length of two chemical repeating units, while PETs(R*-even) had orthorhombic cells with a c axis length of one repeating unit.

The odd-even effects on thermodynamic transition properties are shown in Figures 9a and 9b, which including the S_C* ↔ S_A*, S_A* ↔ TGBA*, and TGBA* ↔ I phase transitions.[25] Figure 9a indicates that the LC phase transitions of PETs(R*-odd) are lower compared with those of PETs(R*-even), and this odd-even effect is stronger in the S_C* phase than those in the S_A* and TGBA* phases. In Figure 9b, the heats of transitions of the S_C* ↔ S_A* and the S_A* ↔ TGBA* also exhibit the identical trends. However, This effect is much stronger in the transition of S_C* ↔ S_A* than that in the S_A* ↔ TGBA* transition. Specifically, in the TGBA* ↔ I transitions the heats of transitions of PETs(R*-odd) are higher than those of PETs(R*-even). It is not clear why this abnormal behavior of the odd-even effect could take place at this moment. One expects that this may be associated with the total atom number of the spacers in the backbones of the polymers and their different packings.

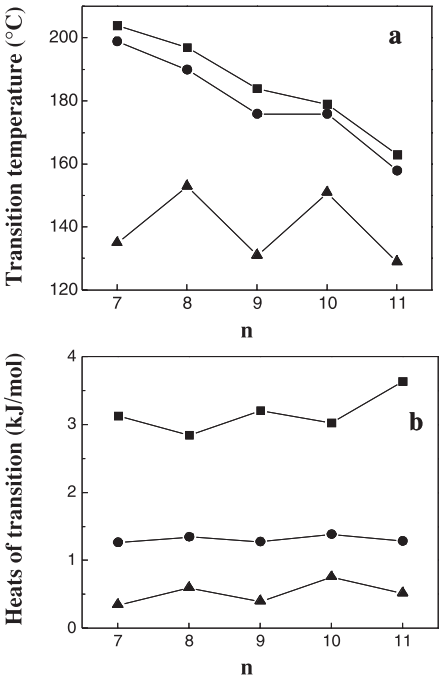

Figure 9. Odd-even effects of the LC phase transition temperatures (a) and heats of transitions for PET(R*-n)s (b): ▲, S_C* ↔ S_A*; ·, S_A* ↔ TGBA*; ■, TGBA* ↔ I.

Conclusion

In summary, phase structural identifications for a non-racemic chiral PET(R*)-n have been carried out. This series of polymers possess complicated LC phase behaviors. In addition to the normal S_A* and S_C* phases, it is the first example for chiral main-chain LC polymers that possesses the TGBA* phase. When crystallization is carried out from the S_A* phase, both the flat-elongated and double-twisted single helical lamellar crystals can be observed. Based on the 2D WAXD pattern and SAED results, the structural analysis can be carried out. This study may serve as an initiation of establishing relationships among structure, morphology and phase transition behaviors of the non-racemic chiral polymers and finding a pathway to connect phase morphology with biomacromolecules. It has also been found that the odd-even effect, caused by the number of methylene units in the backbones in this PET(R*-n) series, not only affected the LC phase transition temperatures and heats of transitions, but also the crystal structures, dimensions, and the handedness of helical lamellar crystals.

Acknowledgement

This work was supported by the NSF (DMR-9617030 and 0203994). CY Li and SZD Cheng also acknowledge the kind of support from PerkinElmer for donating a DSC-7 and supplying a new Diamond DSC in their laboratories at Drexel University and The University of Akron.

References and Notes

1. Janoschek, R. Ed., *Chirality From Weak Bosons to the α-Helix*, Springer-Verlag: Berlin, **1991**.
2. Fujiki, M. *J. Am. Chem. Soc.* **2000**, *122*, 3336-3343.
3. Nelson, J. C.; Saven, J. G.; Moore, J. S.; Wolynes, P. G. *Science* **1997**, *277*, 1793-1796.
4. Cheon, K. .S.; Selinger, J. V.; Green, M. M. *Angew. Chem. Int. Ed.* **2000**, *39*, 1482-1485.
5. Watanabe, J.; Okamoto, S.; Satoh, K.; Sakajiri, K.; Furuya, H. *Macromolecules*, **1996**, *29*, 7084-7088.
6. Li, C. Y.; Cheng, S. Z. D.; Ge, J. J.; Bai, F.; Zhang, J. Z.; Mann, I. .K.; Chien, L. C.; Harris, F. W.; Lotz, B. *J. Am. Chem. Soc.* **2000**, *122*, 72.
7. Li, C. Y.; Yan, D.; Cheng, S. .Z. D.; Bai, F.; He, T.; Chien, L. C.; Harris, F. W.; Lotz, B. *Macromolecules* **1999**, *32*, 524.
8. Li, C. Y.; Yan, D.; Cheng, S. Z. D.; Bai, F.; Ge, J.J.; He, T.; Chien, L. C.; Harris, F. W.; Lotz, B. *Phys. Rev. B* **1999**, *60*, 12675.
9. Li, C. Y.; Cheng, S. Z. D.; Ge, J. J.; Bai, F.; Zhang, J. Z.; Mann, I. K.; Chien, L. C.; Harris, F. W.; Yan, D.; He, T.; Lotz, B. *Phys. Rev. lett.* **1999**, *83*, 4558.
10. Bai, F.; Chien, L. C.; Li, C. Y.; Cheng, S. Z.D.; Percheck, R. *Chem. Mater.* **1999**, *11*, 1666.
11. Ge, J. J.; Honigfort, P. S.; Ho, R. M.; Wang, S. Y.; Harris, F. W.; Cheng, S. Z.D. *Macromol. Chem. Phys.* **1999**, *200*, 31.
12. Pardey, R.; Shen, D.; Gabori, P. A.; Harris, F. W.; Cheng, S. Z. D.; Adduci, J.; Facinelli, J. V.; Lenz, R. W. *Macromolecules* **1993**, *26*, 3687.
13. Pardey, R.; Harris, F. W.; Cheng, S. Z. D.; Adduci, J.; Facinelli, J. V.; Lenz, R. W. Macromolecules 1992, 25, 5060.
14. Yoon, Y.; Zhang, A.; Ho, R..M.; Cheng, S. Z.D.; Percec, V.; Chu, P. *Macromolecules* **1996**, *29*, 294.
15. Yoon, Y.; Ho, R. M.; Moon, B.; Kim, D.; McCreight, K. W.; Li, F.; Harris, F. W.; Cheng, S. Z. D.; Percec, V.; Chu, P. *Macromolecules* **1996**, *29*, 3421.
16. Goodby J. W.; Waugh, M. A.; Stein, S.M.; Chin, E.; Pindak, R.; Patel, J. S. *Nature* **1989**, *337*, 449.
17. Bolton, E. C.; Lacey, D.; Smith, P. J.; Goodby, J. W. *Liq. Cryst.* **1992**, *12*, 305.
18. Geddes, A. J., Parker, K. D., Atkins E. D., Beighton E. *J. Mol. Biol.* **1965**, *11*, 706.
19. Leland, M.; Zhang, A.; Ho, R. M.; Cheng, S. Z. D.; Keller, A.; Kricheldorf, H. R.; *Macromolecules* **1997**, *30*, 5249.
20. Kleman, M; *Physica Scripta* **1987**, *T19*, 565.
21. Kleman, M; *Rep. Prog. Phys.* **1989**, *52*, 555.
22. Livolant, F; Bouligand, Y; *Chromosoma* **1980**, *80*, 97.
23. Li, CY.; Cheng, SZD; Weng, X; Ge, JJ. Bai, F; Zhang, JZ; Calhoun, BH; Harris, FW; Chien, LC; Lotz, B J. *Am. Chem. Soc.* **2001**, *123*, 2462.
24. Lotz, B; Gonthier-Vassal, A; Brack, A; Magoshi, J; *J. Mol. Biol.* **1982**, *156*, 345.
25. Weng, X.; Li, C. Y.; Jin, S.; Zhang, J. Z.; Zhang, D.; Harris, F. W.; Cheng, S. Z. D.; Lotz, B.. *Macromolecules* **2002**, *35*, 9678.

PerkinElmer Life and Analytical Sciences
710 Bridgeport Avenue
Shelton, CT 06484-4794 USA
Phone: (800) 762-4000 or
(+1) 203-925-4602
www.perkinelmer.com

PerkinElmer®
precisely.

006831_01 ELEC0703XX